RESEARCH ARTICLE

Antagonistic Rgg Regulators Mediate Quorum Sensing via Competitive DNA Binding in *Streptococcus pyogenes*

Breah LaSarre,[a] Chaitanya Aggarwal,[b] and Michael J. Federle[b]

Department of Microbiology and Immunology, College of Medicine,[a] and Department of Medicinal Chemistry and Pharmacognosy, Center for Pharmaceutical Biotechnology, College of Pharmacy,[b] University of Illinois at Chicago, Chicago, Illinois, USA

ABSTRACT **Recent studies have established the fact that multiple members of the Rgg family of transcriptional regulators serve as key components of quorum sensing (QS) pathways that utilize peptides as intercellular signaling molecules. We previously described a novel QS system in *Streptococcus pyogenes* which utilizes two Rgg-family regulators (Rgg2 and Rgg3) that respond to neighboring signaling peptides (SHP2 and SHP3) to control gene expression and biofilm formation. We have shown that Rgg2 is a transcriptional activator of target genes, whereas Rgg3 represses expression of these genes, and that SHPs function to activate the QS system. The mechanisms by which Rgg proteins regulate both QS-dependent and QS-independent processes remain poorly defined; thus, we sought to further elucidate how Rgg2 and Rgg3 mediate gene regulation. Here we provide evidence that *S. pyogenes* employs a unique mechanism of direct competition between the antagonistic, peptide-responsive proteins Rgg2 and Rgg3 for binding at target promoters. The highly conserved, shared binding sites for Rgg2 and Rgg3 are located proximal to the −35 nucleotide in the target promoters, and the direct competition between the two regulators results in concentration-dependent, exclusive occupation of the target promoters that can be skewed in favor of Rgg2 *in vitro* by the presence of SHP. These results suggest that exclusionary binding of target promoters by Rgg3 may prevent Rgg2 binding under SHP-limiting conditions, thereby preventing premature induction of the quorum sensing circuit.**

IMPORTANCE **Rgg-family transcriptional regulators are widespread among low-G+C Gram-positive bacteria and in many cases contribute to bacterial physiology and virulence. Only recently was it discovered that several Rgg proteins function in cell-to-cell communication (quorum sensing [QS]) via direct interaction with signaling peptides. The mechanism(s) by which Rgg proteins mediate regulation is poorly understood, and further insight into Rgg function is anticipated to be of great importance for the understanding of both regulatory-network architecture and intercellular communication in Rgg-containing species. The results of this study on the Rgg2/3 QS circuit of *S. pyogenes* demonstrate that DNA binding of target promoters by the activator Rgg2 is directly inhibited by competitive binding by the repressor Rgg3, thereby preventing transcriptional activation of the target genes and premature induction of the QS circuit. This is a unique regulatory mechanism among Rgg proteins and other peptide-responsive QS regulators.**

Received 6 September 2012 **Accepted** 26 October 2012 **Published** 27 November 2012

Citation LaSarre B, Aggarwal C, and Federle MJ. 2012. Antagonistic Rgg regulators mediate quorum sensing via competitive DNA binding in *Streptococcus pyogenes.* mBio 3(6): e00333-12. doi:10.1128/mBio.00333-12.

Editor Bonnie Bassler, Princeton University

Address correspondence to Michael J. Federle, mfederle@uic.edu.

Bacterial cell-to-cell communication, known as quorum sensing (QS), provides bacteria the means to coordinate behaviors across a population. Gram-positive bacteria typically utilize small oligopeptides for intercellular signaling. These peptide pheromones are either detected at the surface of cells by membrane-bound sensor kinases or transported into the cell where they subsequently interact directly with cognate regulators to modulate gene expression (for a review, see reference 1). The major family of proteins responsible for intercellular detection of peptide pheromones is the RNPP family, named for its four prototypical members: Rap, NprR, and PlcR, each found in several *Bacillus* species, and PrgX of *Enterococcus faecalis* (2, 3). Members of the RNPP family are grouped due to their shared secondary structures: each contains a C-terminal region comprised of several tetratricopeptide repeats (TPR), ranging between five and nine repeated motifs among the group (4–6). These motifs are responsible for protein oligomerization and peptide binding (3). NprR, PrgX, and PlcR also contain N-terminal helix-turn-helix (HTH) domains responsible for interactions with DNA (2, 7).

Two well-studied regulators of the RNPP family are PlcR and PrgX. Interestingly, the mechanisms of regulation and effect of peptide differ widely for these two proteins despite their similar structures. PlcR is a *B. cereus* group-specific pleiotropic transcriptional activator of many virulence-related genes (8, 9). Binding of the cognate peptide PapR by PlcR dimers drives intermolecular rearrangements that optimize HTH positioning to align with specific DNA sequences located at target promoters, thus allowing transcriptional activation to occur (2). The gene encoding the PapR peptide is located directly downstream of the *plcR* gene, and PlcR-PapR complexes directly activate transcription of both the

receptor and the peptide genes, generating a positive feedback loop that sustains induction of target genes following initial system activation (10, 11).

In contrast, PrgX is a transcriptional repressor that governs conjugative functions associated with the pCF10 plasmid in *E. faecalis*. PrgX is unique in that it can bind to two distinct peptide pheromones, the chromosomally encoded peptide cCF10, which induces conjugation through disruption of PrgX repression (7), and the pCF10-encoded inhibitor peptide iCF10, which acts as a corepressor and enhances PrgX inhibitory activity (12). Transcriptional repression occurs by a mechanism of DNA looping that is driven by head-to-head interactions between PrgX dimers bound at two DNA sites within in the target promoter of *prgQ* (P_Q) (13). Binding of iCF10 by PrgX promotes this inhibitory loop structure, whereas cCF10 disrupts PrgX tetramers, breaking the DNA loop and allowing RNAP to bind (7, 12). Beyond direct repression by PrgX, transcripts driven from P_Q are also controlled by additional levels of regulation (for a review, see reference 14). These include, in particular, transcriptional interference from the convergent P_X promoter (15). The multiple levels of regulation enable this system to behave as a bistable switch that responds quickly and robustly to conditions favoring conjugation (15). Thus, although RNPP family members have similar structures and bind peptide for function, a full understanding of the QS systems in which they participate has required individual examination of the mechanism by which each protein regulates transcription and responds to peptide.

Recent discoveries have established that a family of proteins apart from the RNPP family, named Rgg, also mediates QS via interaction with signaling peptides (16–21). Rgg proteins, first named for "regulator gene of glucosyltransferase" in *Streptococcus gordonii* (22), are transcriptional regulators that are widespread within low-G+C Gram-positive bacteria, including all streptococcal species as well as *Lactobacillus* and *Listeria* species. Similar to members of the RNPP family, Rgg proteins have an N-terminal HTH motif as well as a C-terminal region predicted to be highly alpha-helical, which is consistent with TPR structures, though bona fide TPR motifs are not identifiable in Rgg proteins using TPR prediction algorithms (23). A number of Rgg proteins have been investigated due to their central roles in the control of important physiological processes (22, 24–38); however, the mechanism(s) of regulation by Rgg-type proteins has not been well characterized. For Rgg proteins that have been investigated, differences in DNA recognition sequences and regulatory activities suggest some degree of mechanistic variation within the family, akin to what has been shown for the RNPP family. For example, the Rgg-type proteins MutR of *Streptococcus mutans* and LasX of *Lactobacillus sakei* appear to function solely as activators (33, 34), whereas RovS of *Streptococcus agalactiae* activates and represses expression of distinct target genes (35).

Because Rgg proteins were not previously known to function as QS regulators, their involvement in cell-to-cell communication has not been widely examined. Genome analysis has revealed that *rgg* genes are often located in the genome adjacent to small open reading frames that encode putative peptides (39). Some of these peptides are small and hydrophobic and have thus been given the name SHP, for "short hydrophobic peptide" (39). The genes encoding SHPs are largely unannotated in sequenced genomes, likely due to their small size, but the prevalence of *rgg-shp* gene associations within *rgg*-containing genomes and the recent evidence of SHP-induced modulation of Rgg function (16, 17, 19) suggest that Rgg proteins comprise a novel category of intercellular QS transcriptional regulators widespread among members of the phylum *Firmicutes*.

Our lab recently described a novel Rgg-based QS system in the Gram-positive, human-restricted pathogen *Streptococcus pyogenes* (group A streptococcus [GAS]) (16). This circuit centers on the antagonistic activity of two Rgg proteins, Rgg2 and Rgg3, which respond to two peptide pheromones, SHP2 and SHP3, to regulate target gene transcription and GAS biofilm biogenesis. Although it has been demonstrated that Rgg2 acts as a transcriptional activator, whereas Rgg3 acts as a repressor of the same target genes, the mechanisms by which these regulatory activities are achieved are unknown.

Herein, we provide mechanistic insight into how the peptide-responsive regulators Rgg2 and Rgg3 function to control QS in GAS. DNA footprinting analysis reveals that both Rgg2 and Rgg3 proteins bind a highly conserved DNA motif present in both *shp* promoters located proximal to the −35 nucleotides. This conserved region is essential for binding, as deletion of the region or mutation of two conserved nucleotides within the motif eliminates *in vitro* Rgg-DNA interactions and *in vivo* transcriptional regulation by Rgg2 and Rgg3. Due to the shared binding sites, only one Rgg protein is able to bind a *shp* promoter at any given time, and *in vitro* studies suggest that SHPs can skew binding of the conserved region in favor of Rgg2. These results support a model wherein Rgg2 binding to the conserved regions functions to induce the QS circuit in a SHP-enhanced manner via a positive feedback loop, whereas Rgg3 binding of the same regions prevents induction of the QS circuit by limiting Rgg2 binding under non-inducing conditions. This is a unique regulatory mechanism and adds to the short list of known system architectures for intracellular peptide-responsive QS systems described to date.

RESULTS

Identification of *rgg* and *shp* transcription start sites and promoter elements. It was demonstrated previously that Rgg2 and Rgg3 activate and repress, respectively, expression of two genes, *shp2* and *shp3*, which encode peptide pheromones capable of inducing biofilm formation in GAS (16). To begin elucidating the mechanism by which these Rgg proteins regulate transcription, we first identified the transcription start sites for both *rgg* and both *shp* genes (Fig. 1A). Rapid amplification of 5′ cDNA ends (5′-RACE) analysis was performed using RNA collected from cells in which the Rgg2/3 system had been induced with a synthetic form of the C-terminal eight amino acids of the SHP3 peptide (sSHP3-C8), which was previously shown to activate the Rgg2/3 QS circuit (16). The transcription start sites for *rgg2* and *rgg3* were 36 nucleotides and 42 nucleotides upstream of their translation initiation codons, respectively (Fig. 1B and C), and for both *rgg* genes there were identifiable −10 and −35 promoter motifs. The transcription start sites for *shp2* and *shp3* were 30 nucleotides and 25 nucleotides upstream of their translation initiation codons, respectively (Fig. 1B and C). Although −10 motifs were present for both *shp* genes, neither promoter contained an identifiable −35 motif with substantial homology to the consensus −35 hexamer sequence (40). Interestingly, proximal to the −35 nucleotide in each *shp* promoter was a conserved region of 23 nucleotides that was identical at 22 of 23 positions (Fig. 1B and C). Given that *shp2* and *shp3* genes are under the same transcriptional regulation by Rgg3

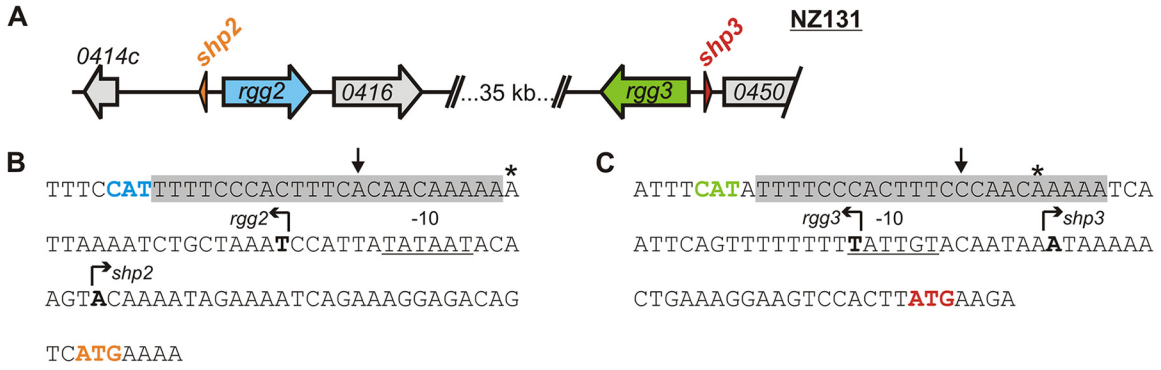

FIG 1 Rgg/SHP pairs in the NZ131 genome (A) and intergenic region maps for *shp2* and *rgg2* (B) and *rgg3* and *shp3* (C) gene pairs. (B and C) Sense DNA strand for the promoter region of each *shp* gene. Translation start codons for Rgg proteins and SHPs are colored to match the gene colors in panel A. Transcription start sites determined by 5′ RACE are in bold, with corresponding bent arrows and gene designations. Predicted −10 promoter elements for the *shp* genes are underlined, and the −35 nucleotides are indicated by asterisks. The conserved region shared between the *shp* promoters is highlighted in gray, with the single nucleotide difference indicated by vertical arrows.

and Rgg2 (16), and that the conserved motifs are positioned where key RNAP-promoter interactions would be expected to occur (for a review, see reference 41), we hypothesized that the conserved regions were important for DNA binding and regulation by Rgg2 and/or Rgg3.

Rgg2 binds the *shp2* and *shp3* promoters *in vitro*. Using untagged purified Rgg3 protein, we previously demonstrated that Rgg3 binds directly to the promoter regions of *shp2* and *shp3 in vitro* (16). Recently, we succeeded in purifying soluble Rgg2 protein fused to an N-terminal maltose binding protein (MBP) tag (MBP-Rgg2) that remained soluble following removal of MBP. The untagged Rgg2 protein was then used in electrophoretic mobility shift assays (EMSAs) to determine its DNA binding activity. Rgg2 was able to bind both the *shp2* and *shp3* promoter regions in a concentration-dependent manner *in vitro*, as visualized by the slower-migrating bands in the presence of protein (Fig. 2A). Additional EMSAs with specific and nonspecific unlabeled competitor DNA and a control rRNA promoter probe that was not shifted in the presence of Rgg2 confirmed the DNA-binding specificity of Rgg2 for the *shp* promoter regions (Fig. 2B). Thus, as previously shown with Rgg3 protein (16), Rgg2 binds directly and specifically to the *shp2* and *shp3* promoters *in vitro*.

Rgg2 and Rgg3 share binding sites in the *shp* promoters that overlap the conserved regions. Although EMSAs demonstrated that Rgg2 and Rgg3 bind directly to the promoters of the *shp* genes (Fig. 2) (16), the precise binding sites for each protein within these regions were unknown. To identify the precise location of binding by Rgg2 and Rgg3, 6-FAM (6-carboxyfluorescein)-labeled DNA probes spanning from −208 to +123 of the *shp2* transcription start site and from −206 to +117 of the *shp3* transcription start site were generated by PCR. These probes were then used in DNase I footprinting reactions, and regions of protection conferred by DNA binding by either Rgg protein were identified using automated capillary electrophoresis. Sites protected from DNase I digestion were visualized as regions lacking discernible peaks compared to a control digest reaction mixture containing bovine serum albumin (BSA). Reaction mixtures containing either Rgg2 or Rgg3 yielded only a single region of protection for all probes tested, indicating the presence of only one Rgg2 or Rgg3 binding site within each *shp* promoter (see Fig. S1 in the supplemental material). Furthermore, both Rgg2 and Rgg3 were found to protect the same region of each probe from DNase I digestion (Fig. 3A). Rgg2 and Rgg3 protected *shp2* sense-strand nucleotides −58 to −39 (Fig. 3B) and *shp3* sense-strand nucleotides −54 to −29 (Fig. 3C), with respect to the *shp* transcription start sites. It is possible that the Rgg-dependent region of protection in the *shp2* promoter extends to the −33 nucleotide, but we were unable to establish the precise boundary of the protected region due to poor digestion of nucleotides −38 to −33 in the control BSA reaction (Fig. 3A). Given the 25-nucleotide region of protection conferred

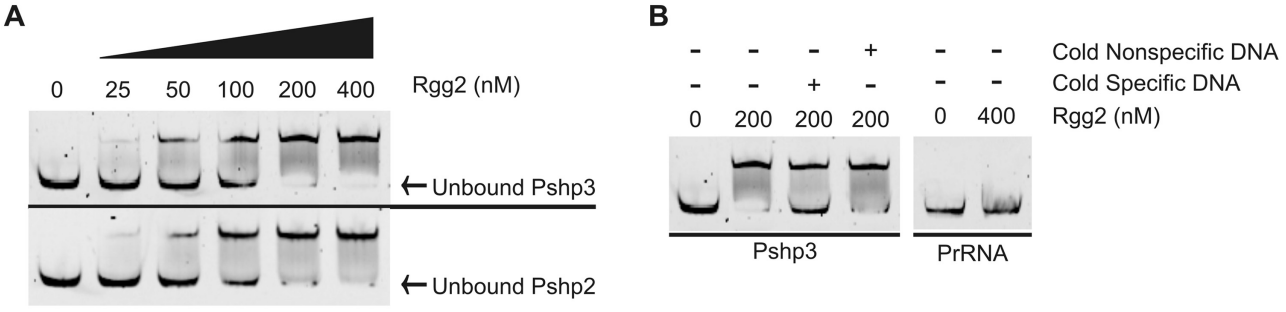

FIG 2 (A) EMSA analysis of Rgg binding to the promoters of *shp3* (top) and *shp2* (bottom) at increasing protein concentrations. (B) EMSA analysis of Rgg2 binding to a control PrRNA probe (right) or the *shp3* promoter in the presence of a 5-fold molar excess of unlabeled specific (P_{shp3}) or nonspecific (PrRNA) competitor DNA (left).

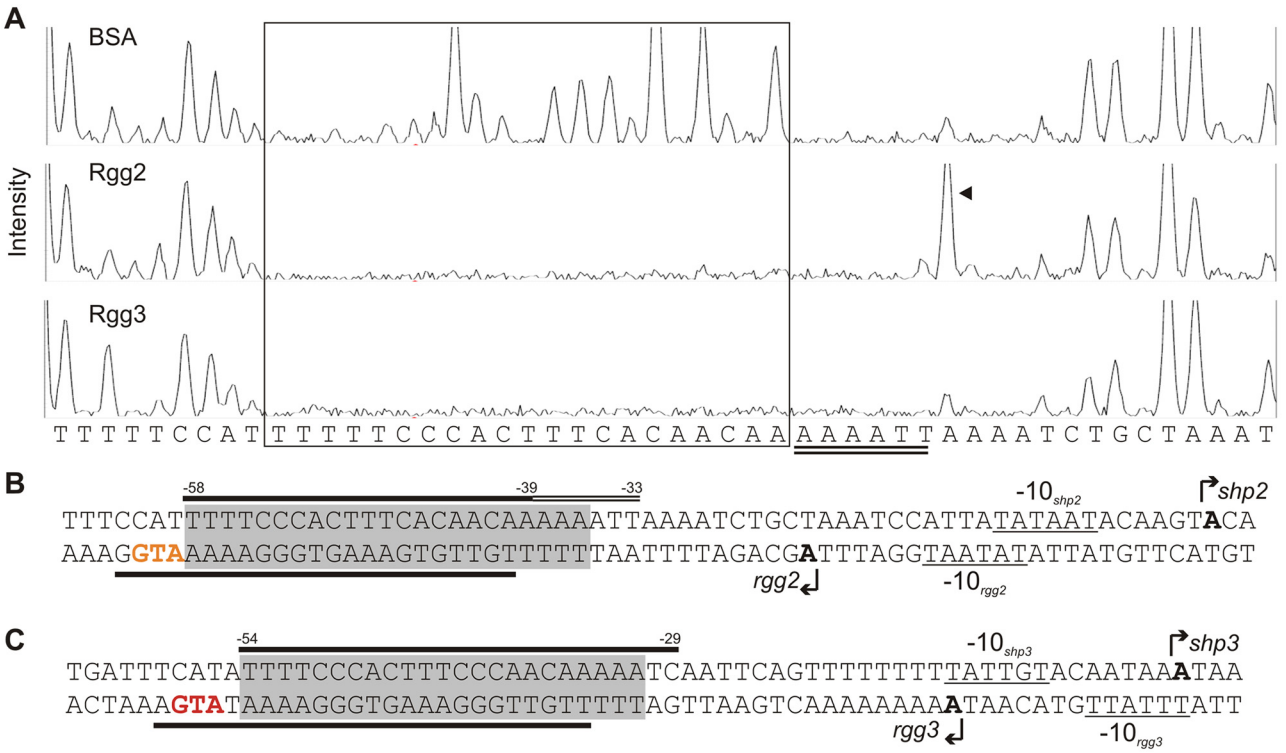

FIG 3 (A) Footprinting electrophoretograms following DNase I digestion of the sense strand of the *shp2* promoter region in the presence of BSA (top), Rgg2 (middle), or Rgg3 (bottom). The box indicates the region of DNA protected by both Rgg proteins, and the corresponding nucleotide sequence is included at the bottom of the panel. Nucleotides possibly protected by Rgg binding are indicated by the double underline. The arrowhead in the Rgg2 panel denotes a hypersensitive site. (B and C) Promoter maps depicting the elucidated Rgg binding sites in the *shp2* (B) and *shp3* (C) promoter regions. Translation start codons for Rgg proteins are colored to match the gene colors in Fig. 1A. Transcription start sites are in bold, with corresponding bent arrows and gene designations. Predicted −10 promoter elements for the *shp* and *rgg* genes are underlined with corresponding designations. The conserved region shared between the *shp* promoters is highlighted in gray, and nucleotides protected during DNase I digestion by Rgg2 and Rgg3 are indicated by horizontal black bars above and below the sense and antisense DNA strand, respectively. The thin double line above nucleotides in the *shp2* promoter corresponds to the possible region of protection indicated by the double underline in panel A.

by the Rgg proteins at the *shp3* promoter, however, it seems likely that the full region of protection in the *shp2* promoter does indeed extend to the −33 nucleotide. For each *shp* promoter, the region of protection on the antisense strand was offset by an average of 5 nucleotides (Fig. 3B and C). Importantly, these Rgg binding sites directly overlap the 23-nucleotide conserved region in each promoter, supporting our hypothesis that the conserved motif serves as a binding site for both Rgg2 and Rgg3. Interestingly, there also appeared to be two DNase I-hypersensitive sites specific for Rgg2, the first at nucleotide −32 on the sense strand of the *shp2* promoter (Fig. 3A) and the other at nucleotide −33 on the antisense strand of the *shp3* promoter (data not shown), suggesting that Rgg2 and Rgg3 may interact with the DNA in slightly different manners despite sharing binding sites.

Conserved region is required for DNA binding and transcriptional regulation by Rgg2 and Rgg3. To confirm the Rgg binding sites identified by DNase I footprinting and their requirement for Rgg-mediated regulation, we investigated the role of the conserved region in DNA binding *in vitro* and the importance of the region for Rgg-mediated regulation *in vivo*. To investigate the requirement of the conserved regions in DNA binding, we performed EMSAs using purified Rgg2 and Rgg3 and various DNA probes of different lengths in which the conserved regions had been included, excluded, or mutated. Binding experiments revealed that both Rgg proteins were unable to bind any probe in which the conserved region was omitted (B probes), indicating that the region was necessary for binding (Fig. 4A and B). Additionally, all probes containing the conserved region (Full, A, and C probes) were bound by Rgg2 and Rgg3, resulting in slower-migrating bands on the EMSA gels (Fig. 4A and B). We also tested the ability of each Rgg protein to bind probes less than 50 nucleotides in length (Pshp2-D and Pshp3-D) that contained the conserved regions but very few additional nucleotides past the experimentally determined Rgg binding sites (Fig. 3). Interestingly, although both of these probes were clearly bound by Rgg3 (Fig. 4A and B, top gels), the binding of these probes by Rgg2 was weak, resulting in a smear of the probes on the gels rather than defined slower-migrating bands (Fig. 4A and B, bottom gels). This suggests that although the experimentally determined binding sites containing the conserved region are sufficient to mediate DNA binding by both regulators, Rgg2 and Rgg3 may interact with DNA in different manners, resulting in weaker interaction of Rgg2 with short DNA sequences under these assay conditions. As a complementary approach to examine the importance of the conserved region for Rgg-DNA interactions, we also generated a mutant probe in which two of the 22 identical nucleotides of the P_{shp2} conserved region were changed (Fig. 4C). Substitution of these two nucleotides was sufficient to disrupt the ability of Rgg2 and

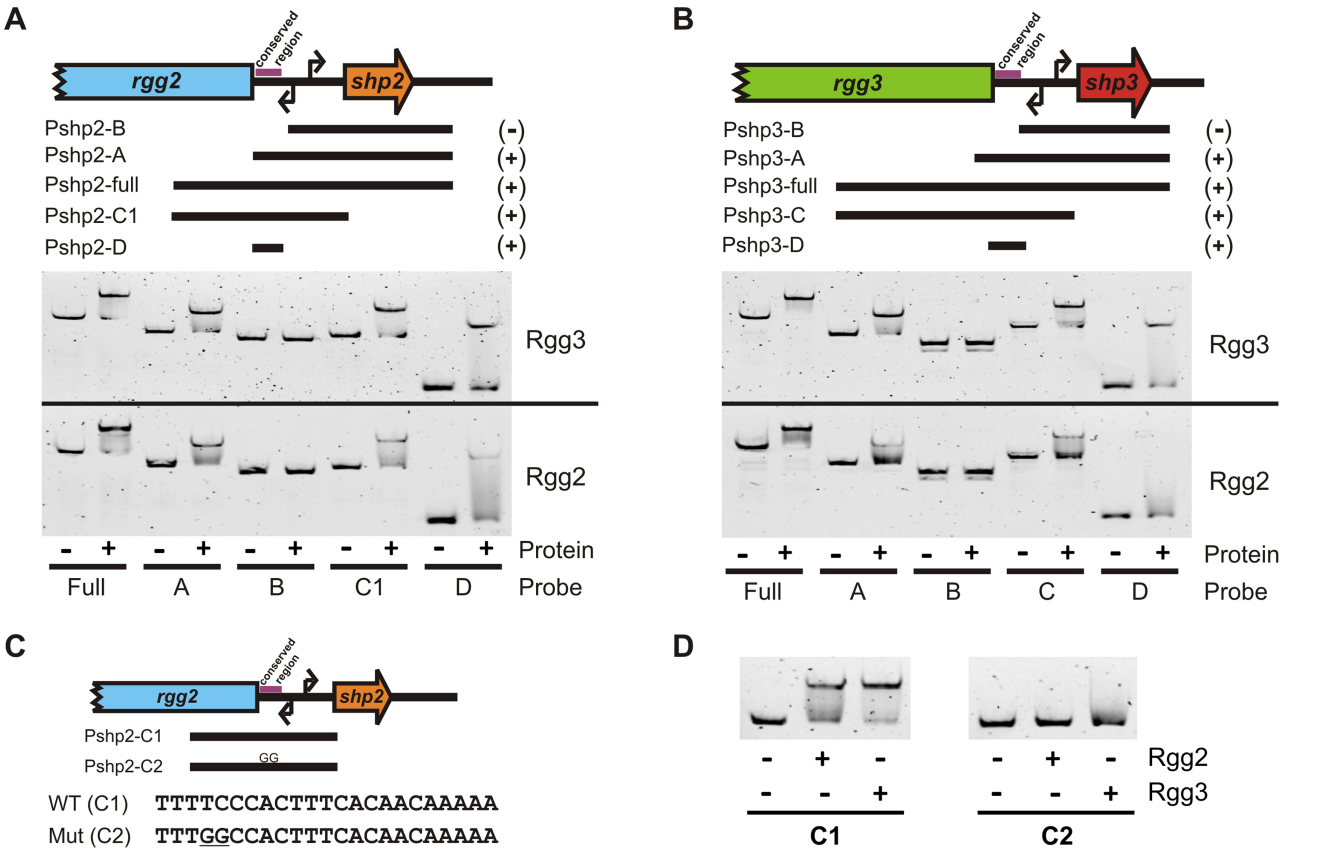

FIG 4 Schematic diagrams of the *shp2* (A) and *shp3* (B) promoter region fragments used as probes in EMSA analyses. Plus and minus signs to the right of each probe indicate the presence or absence of detectable binding of the corresponding probe by Rgg2 and Rgg3. EMSA gels illustrating binding are included below each diagram. (C) Schematic diagram of the *shp2* promoter region and DNA fragments containing the WT (Pshp2-C1) and Mut (Pshp2-C2) conserved region used as probes in EMSA reactions. Nucleotide sequences of the conserved region of each probe are included below, with the two nucleotides changed by site-directed mutagenesis underlined. (D) EMSA analysis of Rgg2 and Rgg3 binding to the Pshp2-C1 and Pshp2-C2 probes. All EMSA reactions were performed using 200 nM Rgg2 or Rgg3.

Rgg3 to bind the DNA (Fig. 4D), further confirming that this region is required for binding by both Rgg proteins. The slight smear of the mutant C2 probe in the presence of Rgg3 but the lack of any visible binding by Rgg2 again suggested that Rgg2 and Rgg3 may have some differential interactions with DNA *in vitro*.

To investigate the role of the conserved region in Rgg-mediated regulation *in vivo*, we generated transcriptional reporters in which the entire intergenic region between *rgg2* and *shp2* (which contains the conserved region; P_{shp2} T1) or a smaller portion of the intergenic region proximal to the *shp2* coding sequence (which excludes the conserved region; P_{shp2} T2) was fused with the genes coding for luciferase (*luxAB*) (Fig. 5A). These reporters were integrated into wild-type (WT) GAS or isogenic Δ*rgg3* and Δ*rgg3* Δ*rgg2* mutants, and luminescence was monitored throughout growth. The activities of these reporters were compared to those in strains carrying a larger reporter (P_{shp2}) in which a 500-bp region upstream of *shp2* was fused to *luxAB*, as this region was previously demonstrated to contain the necessary promoter elements to mediate repression by Rgg3, activation by Rgg2, and response to SHPs (16). The reporter containing the entire intergenic region (P_{shp2} T1) had luminescence expression patterns identical to those of the extended P_{shp2} reporter in WT, Δ*rgg3*, and Δ*rgg3* Δ*rgg2* strains, with light production being repressed in WT strains, expressed highly in the Δ*rgg3* mutant, and absent in the Δ*rgg3* Δ*rgg2* double mutant (Fig. 5B). Additionally, both reporters responded equivalently to synthetic SHPs (data not shown). These data indicate that the intergenic region contains all elements required for Rgg-mediated regulation by SHPs, in agreement with the footprinting results indicating no other Rgg binding sites outside the *rgg2-shp2* intergenic region. Importantly, the shortest reporter in which the conserved region was omitted (P_{shp2} T2) did not generate detectable luminescence in Δ*rgg3* mutant (Fig. 5B), and was not induced by the addition of synthetic peptide (data not shown). These data confirmed the importance of the conserved region for Rgg-mediated regulation *in vivo* and indicated that the promoter elements between the conserved region and the *shp2* gene are not sufficient for RNAP recruitment, as there was no detectable expression of the P_{shp2} T2 reporter in any strain (Fig. 5B). To further verify the necessity of the conserved region for *in vivo* regulation by the Rgg proteins, we also generated an additional version of the P_{shp2} T1 reporter in which the two nucleotides shown to be important for *in vitro* binding by Rgg2 and Rgg3 (Fig. 4C) were mutated to GG (P_{shp2} mutT1). Unlike the P_{shp2} T1 reporter, which carries the wild-type consensus sequence, the P_{shp2} mutT1 reporter did not generate detectable luminescence in any strain (Fig. 5C), validating the *in vitro* binding results and bolstering our

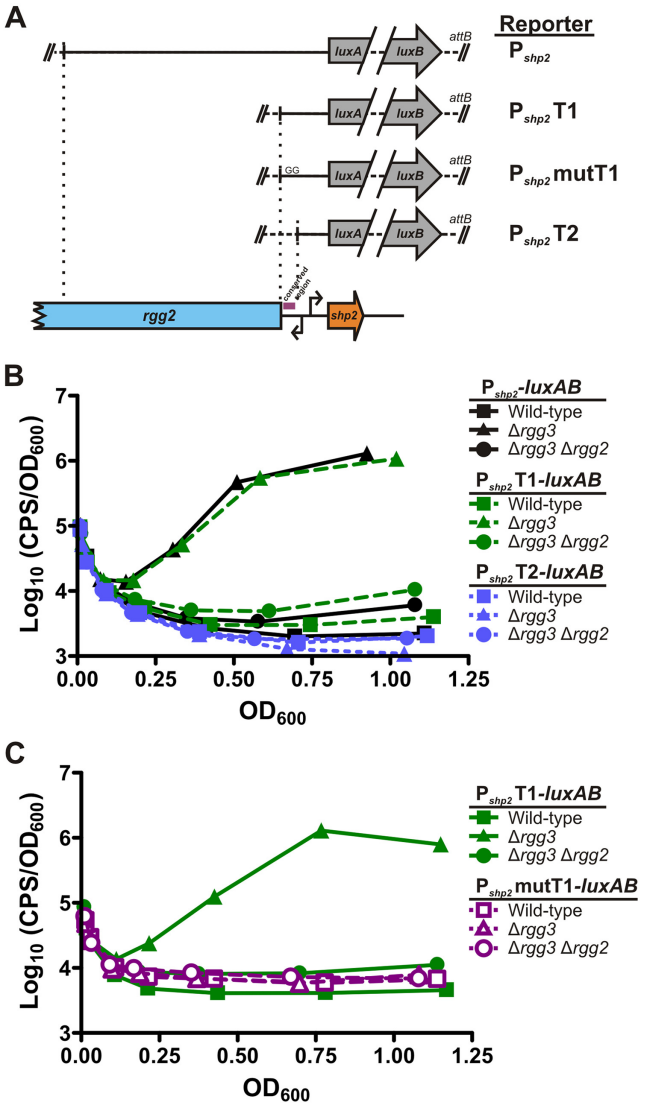

FIG 5 (A) Schematic diagram of DNA fragments containing various segments of the *shp2* promoter used in transcriptional fusions with *luxAB* (P_{shp2}, pBL111; P_{shp2} T1, pBL116; P_{shp2} mutT1, pBL118; P_{shp2} T2, pBL117). P_{shp2} mutT1 is identical to the P_{shp2} T1 reporter except that two nucleotides in the conserved region have been mutated as shown in Fig. 4C. (B) Luciferase expression from P_{shp2}, P_{shp2} T1, and P_{shp2} T2 reporters integrated into WT (BNL148, BNL172, and BNL179), Δ*rgg3* (BNL149, BNL173, and BNL180), and Δ*rgg3* Δ*rgg2* (BNL153, BNL189, and BNL190) strains grown in CDM (chemically defined medium). (C) Luciferase expression from P_{shp2} T1 and P_{shp2} mutT1 reporters in WT (BNL148 and BNL181), Δ*rgg3* (BNL149 and BNL182), and Δ*rgg3* Δ*rgg2* (BNL153 and BNL183) strains grown in CDM. All luminescence data shown are representative of at least 3 independent experiments.

conclusion that the conserved region is required for Rgg-mediated regulation.

Rgg2 and Rgg3 directly compete for binding of target promoters. Given that Rgg2 and Rgg3 share a binding site in each *shp* promoter, it was not surprising that there was no detectable simultaneous binding of any DNA probe when both proteins were incubated together with the DNA, which would be visualized as a supershift of the probe compared to binding by either protein alone (data not shown). Due to the comparable molecular weights of purified Rgg2 and Rgg3 (34.452 kDa and 34.069 kDa, respectively), slower-migrating bands resulting from Rgg2 and Rgg3 binding are positioned equivalently on the gel, precluding direct identification of the protein responsible for the shift when both proteins are added to a single EMSA reaction. We found, however, that purified MBP-Rgg2 retaining the MBP tag exhibited DNA binding activity comparable to that of Factor Xa-treated Rgg2 (see Fig. S2 in the supplemental material). Since MBP-Rgg2 is nearly double the size of Rgg2 (76.916 kDa versus 34.452 kDa), DNA binding by MBP-Rgg2 results in a more slowly migrating band that is clearly distinguishable from that resulting from Rgg2 binding (see Fig. S2 in the supplemental material). We thus decided to use MBP-Rgg2 in co-EMSAs with Rgg3 to assess competition between the two proteins for DNA binding at the shared binding site.

When purified MBP-Rgg2 and Rgg3 proteins were incubated together with DNA, the direct competition of the two proteins for binding of the DNA was observable, with distinct bands evident for DNA bound by each protein individually and no additional higher bands that would correspond to simultaneous binding of the DNA (Fig. 6A). The absence of intermediate bands between those of the MBP-Rgg2- and Rgg3-DNA complexes also indicated that the two proteins do not form functional heterodimers *in vitro*, although multiple Rgg proteins are known to form homodimers (reference 42 and our unpublished results). The native intracellular concentrations of Rgg2 and Rgg3 are currently unknown; thus, it is not possible at this time to know the proper concentration of each protein to use in the EMSA reactions to mimic the physiological state within the cell. In light of this, we chose to examine binding under a range of different Rgg2 and Rgg3 concentrations. We found that when concentrations of MBP-Rgg2 and Rgg3 were equivalent, the amounts of probe bound by the proteins were comparable (Fig. 6A). This is in agreement with titration studies showing that both proteins bind *shp* promoter DNA with similar affinities (Fig. 2) (16). In contrast, when the concentrations of the two proteins differed, the binding of the probe was skewed in favor of the more abundant protein in all cases (Fig. 6A). This indicates that an alteration in intracellular protein concentrations could directly affect *shp* expression due to skewed promoter binding by Rgg2 and Rgg3.

Given that addition of synthetic SHPs to WT cultures activates the Rgg2/3 QS system (16), we hypothesized that SHPs may stimulate system activation by altering the occupation of the *shp* promoter binding sites to allow the formation of Rgg2-DNA complexes. To mimic the cellular state of uninduced WT GAS in which *shp* gene expression is repressed, we set up EMSA reaction mixtures containing 400 nM Rgg3 and 200 nM MBP-Rgg2. Under these conditions, Rgg3-DNA interactions are favored due to the higher abundance of Rgg3 in the system, and only a faint MRP-Rgg2-DNA band is visible (Fig. 6A and B). We then tested the ability of sSHP-C8 peptides to alter the competitive DNA binding by Rgg3 and MBP-Rgg2. In agreement with our hypothesis, addition of sSHP3-C8 to these EMSA reaction mixtures was sufficient to skew binding such that MBP-Rgg2-DNA interactions were enhanced (Fig. 6B). sSHP3-C8-induced biasing of DNA-binding in favor of MBP-Rgg2 was also detectable when overall lower concentrations of protein were used (see Fig. S3 in the supplemental material). Limited MBP-Rgg2-DNA interactions were detectable in the absence of peptide or when a control sSHP3-revC8 peptide was added. In contrast to sSHP3-C8, sSHP2-C8 failed to readily enhance MBP-Rgg2-DNA interactions (Fig. 6B; also, see Fig. S3 in

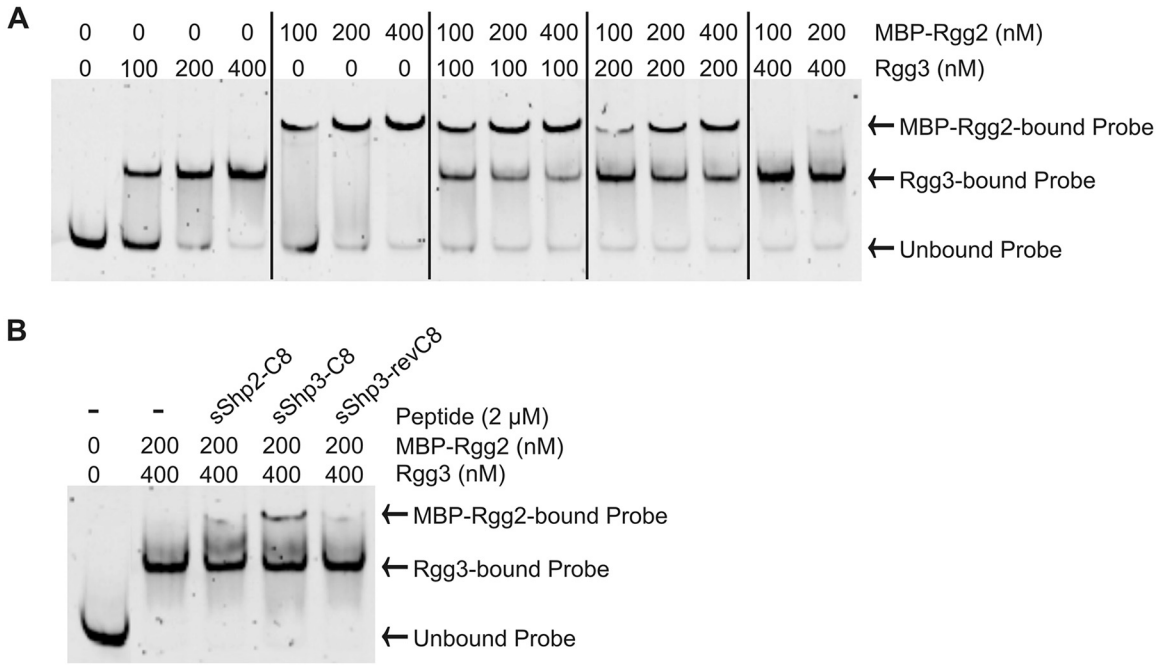

FIG 6 (A) Co-EMSA analysis of competitive DNA binding by MBP-Rgg2 and Rgg3 using various protein concentrations. (B) Co-EMSA analysis of competitive DNA binding by Rgg proteins in the presence of pure (>95%) sSHP-C8 peptides. sSHP3-revC8 was included as a control. All reaction mixtures contained 10 nM Pshp3 probe.

the supplemental material), although this was not unanticipated given the observed difference in activities of sSHP2-C8 and sSHP3-C8 in disruption of Rgg3-DNA interactions *in vitro* (see Fig. S4 in the supplemental material) (16). Despite that SHPs were previously implicated in promoting Rgg2-mediated activation *in vivo* (16), we were unable to observe any reproducible, peptide-driven enhancement of the binding affinity of MBP-Rgg2 or Rgg2 for DNA *in vitro* in the absence of Rgg3 (see Fig. S5 in the supplemental material). We were, however, able to detect direct interactions between MBP-Rgg2 and both sSHP2-C8 and sSHP3-C8 peptides as determined by fluorescence polarization (see Fig. S6 in the supplemental material). There was no detectable interaction with a control peptide (see Fig. S6 in the supplemental material), and MBP alone was not able to interact with any peptide tested (data not shown). Taken together, the peptide-induced DNA-binding responses of Rgg3 and MBP-Rgg2 individually and in competition suggest that SHP can promote dissociation of Rgg3-DNA complexes, which liberates free DNA that is then accessible to Rgg2, thereby indirectly enhancing Rgg2-DNA interactions under these conditions. The mechanism(s) by which direct Rgg2-SHP interactions contribute to system activation remains to be elucidated but appears to be independent of DNA binding.

DISCUSSION

The Rgg family of transcriptional regulators is widespread among the low-G+C Gram-positive bacteria but has only recently been shown to include members whose functions are modulated by peptide pheromones. Since Rgg proteins are a relatively newly recognized family of intracellular peptide-binding receptors, the mechanistic understanding of Rgg-mediated regulation in the context of QS remains in its infancy. Here we provide evidence that the pheromone-responsive Rgg-type regulators Rgg2 and Rgg3 directly compete with each other for binding at target promoters in GAS. Various *in vitro* and *in vivo* studies demonstrate that Rgg2 and Rgg3 recognize a shared binding site in the *shp* promoters that is required for both Rgg2-mediated activation and Rgg3-mediated repression of target genes. Furthermore, this direct competition results in concentration-dependent, exclusive occupation of the target promoters that can be skewed in favor of Rgg2 *in vitro* by the presence of SHP. These results support a model wherein Rgg3 occupation of the shared binding site prevents transcriptional activation of the *shp* genes by inhibiting Rgg2 binding under SHP-limiting conditions, thereby preventing premature robust induction of the QS circuit, and wherein SHPs bias Rgg-DNA interactions in a way that supports Rgg2 engagement of target gene promoters, consequently triggering system activation.

Based on the location of binding relative to the −35 and −10 promoter elements, transcriptional activator proteins are classically labeled as type I or type II activators. Type I activators bind upstream of the −35 element and activate transcription through favorable interactions with the α-subunit C-terminal domain of RNAP. In contrast, type II activator binding sites partially or, in rare instances, fully overlap the −35 promoter element, and the activator interacts with region 4 of the sigma subunit of RNAP to promote transcription (for reviews, see references 41 and 43). Because the Rgg binding sites identified herein partially and fully overlap the −35 regions of the *shp2* and *shp3* promoters, respectively, we propose that Rgg2 functions as a type II activator protein. The lack of detectable expression from transcriptional reporters in Δ*rgg3* Δ*rgg2* strains (Fig. 5) indicates that the lack of a −35 element in the *shp* promoters hinders activator-independent transcription and that protein-protein interactions between Rgg2 and RNAP may substitute functionally for the −35 element in RNAP recruitment. Several other Rgg proteins have also been

found to bind target promoters near the −35 region, although the precise binding recognition sequences by Rgg2 and Rgg3 are not highly homologous to those of other Rgg proteins (17, 34). Still, it may be that type II activation is a shared mechanism among Rgg-type transcriptional activators.

Separately, the ability of Rgg3 to directly inhibit Rgg2-DNA interaction via exclusive engagement of the shared binding site indicates that Rgg3 represses *shp* gene transcription through steric interference. This is distinct from the mechanism of repression of PrgX, the only other known peptide-binding transcriptional repressor protein, in several ways: Rgg3 binds only one site within each target gene promoter, no DNA looping appears to be involved in the Rgg2/3 circuit, and the PrgX system lacks a competitive activator protein comparable to Rgg2. Given that expression from the *shp* promoters is highly induced in the absence of Rgg3 without any addition of exogenous peptide (Fig. 5), the Rgg3-mediated steric interference of Rgg2 binding appears to be important for prevention of premature QS system activation. We speculate that the relative concentrations of Rgg2 and Rgg3 in the cell under low-peptide conditions likely favor Rgg3 engagement of the *shp* promoters, given that Rgg2 can readily compete with Rgg3 for binding when concentrations of the two proteins are equivalent or Rgg2 is in abundance (Fig. 6). This is in agreement with previous experiments demonstrating that overexpression of Rgg2 from a plasmid can activate the QS system even in the presence of Rgg3 (16).

The spatial organization of the *rgg* and *shp* promoters within each intergenic region also deserves discussion. For each *rgg-shp* gene pair, the predicted promoter elements partially overlap (Fig. 3B and C), which could result in transcriptional interference (44). Regulation via transcriptional interference is not unprecedented within QS systems, as such interference by colliding RNAP complexes originating from the convergent P_Q and P_X promoters is integral to successful maintenance of the bistable switch in the PrgX system (15). The P_Q and P_X promoters, however, are much further apart than the P_{rgg} and P_{shp} promoters, so interference in the Rgg2/3 system would likely result from promoter competition rather than RNAP collisions, given that there is no overlap in the *rgg* and *shp* transcripts themselves. If such interference is at play, an increase in expression of the *shp* genes would theoretically cause a decrease in *rgg* gene expression. Preliminary work in our lab suggests that this type of transcriptional interference may take place, but the magnitude of the effect is no more than 2-fold (our unpublished results). Intriguingly, given that each *rgg* promoter similarly overlaps an adjacent *shp* promoter, transcriptional interference would be expected to decrease expression of both *rgg* genes, potentially maintaining the Rgg2-to-Rgg3 ratio within the cell amid an overall decline in absolute Rgg levels.

It has been established that in the absence of *rgg3*, the Rgg2/3 system is activated in an Rgg2-dependent manner and results in high level expression from the *shp* promoters (Fig. 5B) (16). It was also shown previously that deletion of *shp3* in the Δ*rgg3* mutant strain abolished system activation, signifying that removal of *rgg3* is not sufficient and that SHPs, or at least SHP3, are required for Rgg2-mediated system activation *in vivo* (16). Furthermore, data presented herein demonstrate that MBP-Rgg2 directly interacts with both sSHP-C8 peptides *in vitro* (see Fig. S6 in the supplemental material), suggesting that SHPs directly influence Rgg2 activity. We were therefore surprised to find that purified Rgg2 protein had DNA binding activity *in vitro* in the absence of SHPs (Fig. 2) and addition of sSHPs had no discernible effect on this activity (see Fig. S5 in the supplemental material). There are several plausible explanations for this discrepancy. First, the interaction of Rgg2 with peptide may induce a conformational change in Rgg2 that is necessary for productive interaction with RNAP but that is not required for DNA binding, akin to the proposed mechanism for Rgg1358, where *in vitro* DNA binding was not affected by a cognate peptide despite peptide-mediated induction *in vivo* (17). Second, the experimental conditions used to purify soluble Rgg2 may push Rgg2 to adopt a conformation that favors DNA binding independent of SHP peptide. Third, Rgg2 protein stability *in vivo* may be dependent on interaction with SHPs, in which case the purification of soluble MBP-Rgg2 protein from *Escherichia coli* may inherently bypass a GAS-specific SHP-dependent stabilization process that contributes to Rgg2 activity. Our difficulty in purifying soluble Rgg2 using other tags and conditions suggests that Rgg2 is unstable in *E. coli* which may reflect native protein instability in GAS. Further experiments are under way to investigate these possibilities.

Sequence comparison of Rgg2 and Rgg3 suggests a structural basis for the antagonistic regulatory activities and shared DNA binding sites of these regulators. The full-length Rgg2 and Rgg3 proteins are 55% identical and 75% similar on the amino acid level (95% coverage), which is quite high compared to sequence similarity between other Rgg proteins (34, 36, 38). The putative HTH domains of Rgg2 and Rgg3 (amino acids 1 to 64) share 71% identity and 94% similarity (98% coverage), which is apparently sufficient to allow recognition of the same binding sites. Meanwhile, the differences between the two HTH domains may account for slight variations in binding by the two proteins, such as the reduced ability of Rgg2 to bind shorter EMSA probes than that displayed by Rgg3 (Fig. 4A and B). In contrast to the HTH domains, the C-terminal regions of the proteins, which are hypothesized to be involved in protein oligomerization and peptide binding based on predicted structural similarity to PlcR (20), are only 52% identical and 72% similar (90% coverage). If these domains indeed mediate protein oligomerization, relative positioning of the HTH domains within the oligomers may vary between Rgg2 and Rgg3, which could also factor into differences in DNA binding. Separately, we hypothesize that the distinct C-terminal domains are responsible for the antagonistic regulatory activities of Rgg2 and Rgg3 due to differential interactions with RNAP.

On a final note, an Rgg protein from *S. agalactiae*, RovS (Gbs1555), is 80% identical and 88% similar to Rgg2 on the amino acid level (96% coverage) and is encoded divergently from a *shp* gene encoding a peptide identical to SHP2 except for an isoleucine that has replaced the valine residue at position 3. Additionally, the intergenic region between *rovS* and the *shp* gene is 88% identical to the *rgg2-shp2* intergenic region and includes the first 20 nucleotides of the conserved region demonstrated herein to function in Rgg2 binding. Unfortunately, only putative virulence-associated genes have been examined for regulation by RovS (3); thus, it remains unknown if RovS indeed regulates the adjacent *shp* gene, as would be predicted based on its overall homology with *rgg2-shp2*. Interestingly, in contrast to Rgg2, which appears to function solely as an activator (reference 16 and our unpublished results), RovS has been found to be an activator and a repressor of different target genes (35). The HTH domains of RovS and Rgg2 are 94% identical and 98% similar (amino acids 1 to 64), which would suggest that they recognize homologous binding sites; however,

the proposed consensus sequence for RovS (AWAAWVHTDAW-$N_{6/7}$-WTKWWAMDWAK) (35) does not share strong homology with the Rgg2 binding sites identified herein (Fig. 3). Additionally, the only experimentally mapped binding site for RovS lies 111 to 139 bp upstream of the transcription start site of the RovS-repressed gene *fbsA*, much more distant than the binding sites of Rgg2 and Rgg3 from the *shp* transcription start sites (Fig. 3). Elucidation of the structural variations between Rgg2, Rgg3, and RovS that contribute to these mechanistic differences may prove useful in further identifying general features of Rgg proteins important for regulatory functionality.

MATERIALS AND METHODS

Bacterial strains and media. GAS was grown in Todd-Hewitt medium (TH; BD Biosciences) supplemented with 2% (wt/vol) yeast extract (Y; AMRESCO) or in chemically defined medium (CDM) (16) containing 1% (wt/vol) glucose. When necessary, antibiotics were included at the following concentrations: chloramphenicol (Cm), 3 μg ml^{-1}; erythromycin (Erm), 0.5 μg ml^{-1}; spectinomycin (Spec), 100 μg ml^{-1}. *E. coli* strains DH10β (Invitrogen) and BH10C (45) were used for cloning and were grown in Luria broth (LB) or on Luria agar with antibiotics at the following concentrations: chloramphenicol, 10 μg ml^{-1}; erythromycin, 500 μg ml^{-1}; spectinomycin, 100 μg ml^{-1}. The *E. coli* expression strain C41(DE3) (46) was maintained on LB agar with ampicillin at 100 μg ml^{-1}. All bacterial strains used in this study are described in Table S1 in the supplemental material.

Construction of plasmid templates and site-directed mutagenesis of the conserved region. All plasmids and primers used in this study are described in Tables S2 and S3, respectively, in the supplemental material. Regions of approximately 600 bp encompassing *shp2* or *shp3* and their promoters were amplified from NZ131 genomic DNA using primer pairs BL43/SHP2-C9-REV and JC174/JC175, respectively. These regions were then digested with appropriate enzymes and ligated into pLZ12Sp to generate pBL113 and pBL114 for use as PCR templates. To generate a plasmid template in which two nucleotides within the P_{shp2} conserved region were mutated (pBL115), BL73 and BL74 primers were used in an inverse PCR with pBL113 as the template, and plasmids carrying the desired mutation were identified by sequencing.

Construction of *luxAB* reporters. Construction of transcriptional reporters followed the general method used to construct pBL111 as described by Chang et al. (16), with some modifications. Briefly, regions of the *shp2* promoter either containing or omitting the conserved region were amplified from pBL113 using primer pair BL75/BL44 or BL76/BL44, respectively. These products were then ligated at their SalI site to the *cat* terminator which was amplified from pEVP3 using primers BL78/BL79. The terminator-promoter fusions were subsequently amplified from the ligation reactions by PCR using primers BL78/BL44. Separately, the *Vibrio fischeri luxAB* genes were amplified from pCN59 (47) using primers BL26/BL28. The terminator-promoter fusions were then fused in-frame to *luxAB* by overlap extension PCR using primers BL78/BL27. The reporter fusion products were ligated into the BamHI and EcoRI sites of p7INT to generate pBL116 and pBL117. To generate pBL118, containing two nucleotide mutations in the conserved region, the protocol was as described above except that the *shp2* promoter was amplified by PCR using primers BL77/BL44 and pBL115 as the template. All reporter plasmids were electroporated into GAS, and site-specific integration of the plasmids at a $tRNA^{Ser}$ gene was confirmed by PCR.

Luminescence transcriptional reporter assays. Luminescence assays were performed as described by Chang et al. (16). Briefly, overnight cultures were diluted 100-fold into CDM and incubated at 37°C. Throughout growth the optical density of the culture at 600 nm (OD_{600}) was measured using a Spectronic 20D spectrophotometer (Milton Roy), and luminescence (counts per second [CPS]) of 50-μl culture aliquots was quantified using a Wallac 1450 Microbeta scintillation counter. In experiments containing synthetic peptides, strains were grown to mid-log phase in CDM and were then diluted 1:12 into fresh CDM containing a 50 nM concentration of the peptide of interest.

Synthetic peptides. Unlabeled or N-terminal fluorescein isothiocyanate (FITC)-labeled synthetic peptides were purchased from Neo-Peptide (Cambridge, MA) as pure preparations (>95%). The amino acid sequence of FITC-labeled control peptide 2040-C8 is ADLAYQSA. A crude preparation of sSHP3-C8 (34.26% pure) was used for induction of strain NZ131 in identification of transcription start sites as described below. Synthetic peptides were reconstituted as 2 mM (unlabeled peptides) or 1 mM (FITC-labeled peptides) stocks in dimethyl sulfoxide (DMSO) and stored at −80°C.

Identification of transcription start sites. NZ131 was grown to an OD_{600} of 0.325, at which point the cells were transferred to CDM containing 50 nM sSHP3-C8. Following incubation at 37°C for 45 min, RNA was harvested from the cells using a RiboPure bacterial kit (Ambion) following the manufacturer's instructions. RNA quality was confirmed by agarose gel electrophoresis. Transcription start sites for *rgg2*, *rgg3*, *shp2*, and *shp3* were determined using a 5′ RACE kit (Invitrogen) according to the manufacturer's instructions. The GSP1 and GSP2 primers used for each transcript were as follows: rgg2-RACE-1 and rgg2-RACE-2 (*rgg2*), rgg3-RACE-1 and rgg3-RACE-2 (*rgg3*), shp2-RACE-1 and shp2-RACE-2 (*shp2*), and shp3-RACE-1 and shp3-RACE-2 (*shp3*).

Purification of recombinant Rgg3. Recombinant His6-Sumo-Rgg3 protein was purified from *E. coli* by affinity chromatography as previously described (16). Untagged Rgg3 was subsequently obtained by treatment of the recombinant protein with Sumo protease and additional affinity chromatography to remove the His6-Sumo tag as previously described (16). All *in vitro* experiments were carried out using untagged Rgg3 protein.

Purification of recombinant MBP-Rgg2 and factor Xa treatment. The *rgg2* gene (*spy49-0415*) from GAS strain NZ131 was PCR amplified using primers MBP-Rgg2-Fwd and MBP-Rgg2-Rev and cloned into the pMal-c2 vector (NEB, Inc.) at HindIII and EcoRI sites, generating a fusion with MBP at the Rgg2 N terminus. This plasmid (pCA104) was transferred to *E. coli* C41(DE3) for protein expression. Bacteria were grown in ampicillin-supplemented LB medium at 37°C until OD_{600} 0.6 and induced with 0.5 mM isopropyl-D-1-thiogalactopyranoside (IPTG) for 6 h at 30°C. Cells were lysed by sonication in buffer A (20 mM Tris-HCl, 200 mM NaCl, 1 mM EDTA, 10 mM β-mercaptoethanol) containing 0.1 mg/ml lysozyme, 0.01 mg/ml DNase I (Sigma-Aldrich) and Complete protease inhibitor (Roche Molecular Biomedicals). Lysates were cleared by centrifugation at 45,000 × *g* for 20 min at 4°C followed by filtration through a 0.2-μm polyvinylidene fluoride (PVDF) syringe filter (Millipore Corp.). Cleared lysate was loaded on to 5 ml amylose resin (NEB), washed with 12 column volumes (CV) of buffer A, and eluted with 2 CV of buffer A plus 10 mM maltose. Fractions containing MBP-Rgg2 were pooled and concentrated using a 50,000-molecular-weight-cutoff (MWCO) spin filter (Millipore Inc.). Protein concentration was estimated by OD_{280} using a NanoDrop spectrophotometer (Thermo Scientific), and recombinant protein appeared to be >90% pure by Coomassie staining of the SDS-PAGE gel. MBP-Rgg2 was stored in buffer A with 20% glycerol at −80°C. Immediately prior to use in EMSA and DNase I protection assays, MBP-Rgg2 was treated with 5% (wt/wt) factor Xa (NEB) in buffer A containing 20% (vol/vol) glycerol for 18 h at room temperature. Untreated MBP-Rgg2 was used for certain EMSAs, as described in the text.

EMSA. EMSA probes were generated by PCR using pBL113 or pBL115, pBL114, and NZ131 DNA as templates for P_{shp2}, P_{shp3}, and P_{rRNA} probes, respectively. Selected primers included FAM fluorescent tags (Integrated DNA Technologies) at their 5′ ends. The following EMSA probes were amplified with the primers given in parentheses: *Pshp2* full (BL50/BL52), *Pshp2* A (BL55/BL53), *Pshp2* B (BL54/BL53), *Pshp2* C1 and C2 (BL50/BL56), *Pshp3* full (BL65/BL66), *Pshp3* A (BL60/BL66), *Pshp3* B (BL61/BL66), *Pshp3* C (BL65/BL62), and *PrRNA* (BL35/BL37). Unlabeled versions of *Pshp2* full, *Pshp3* full, and *PrRNA* for use as competitor DNA were generated in the same manner using primers BL51, BL68, and BL36

in place of BL50, BL65, and BL37, respectively. EMSA probes <50 nucleotides in length (*Pshp2* D and *Pshp3* D probes) were generated *in vitro* by annealing high-pressure liquid chromatography (HPLC)- or PAGE-purified oligonucleotide pairs BL57/BL58 and BL63/BL64 in 50 mM Tris (pH 7.5), 100 mM NaCl and gradually cooling from 95°C to 15°C over 160 min. Annealed DNA probes were treated with exonuclease I (NEB) to eliminate any residual single-stranded oligonucleotides prior to use in EMSAs.

EMSA experiments were performed as described previously by Chang et al. (16) with modifications. Briefly, recombinant Rgg3 and/or Rgg2 was incubated in reaction mixtures containing 20 mM HEPES, pH 7.9; 20 mM KCl; 5 mM $MgCl_2$; 0.2 mM EDTA, pH 8.0; 0.5 mM dithiothreitol; 50 μg ml^{-1} sheared DNA (AMRESCO); 0.001 U μl^{-1} poly(dI·dC); 100 μg ml^{-1} bovine serum albumin; 0.5 mM $CaCl_2$; and 12% (vol/vol) glycerol. Following the addition of 10 nM probe, reaction mixtures were incubated at room temperature for 30 min. Competitor DNA, when included, was added to a final concentration of 50 nM simultaneously with the labeled probe. Reactions using mixtures containing SHPs followed the same protocol as above except that 2 μM synthetic peptide, or DMSO for reactions omitting peptide, was added 20 min after addition of the probe. For co-EMSAs and EMSAs containing peptides, sample aliquots of 6 μl were separated on 15-well 5% native polyacrylamide gels buffered with 20 mM potassium phosphate, pH 7.5, and run for 60 min at 100 V and 4°C. For all other EMSAs, 8-μl sample aliquots were separated on 10-well gels under the same conditions but run for 40 min at 100 V at 4°C. All gel shifts were detected by fluorescence imaging using a Typhoon phosphorimager (GE Life Sciences).

DNase protection assay. DNase footprinting experiments were performed using automated capillary electrophoresis as previously described (48). Plasmids pBL113 and pLB114 were used as PCR templates to generate fluorescently labeled probes using primer pairs BL65/BL66 and BL67/BL68 (*shp2* fragment) and BL69/BL70 and BL71/BL72 (*shp3* fragment), respectively. For each PCR, only one of the two primers used was 5′ FAM labeled, resulting in four labeled probes in total, each uniquely labeled at the 5′ end of one strand. All probes were purified by native polyacrylamide gel electrophoresis (PAGE) prior to use in protection assays. Binding reactions using 40-μl binding reaction mixtures containing 400 nM recombinant Rgg3 or Rgg2 and 10 nM probe were performed as described for EMSA, except that sheared DNA and poly(dI·dC) were omitted. Control reactions were performed using the same binding protocol but with equimolar amounts of BSA used in place of Rgg protein. Based on results from optimization experiments, all complexes were partially digested with 0.1 U DNase I (NEB) at room temperature for 3 min, and reactions were terminated by the addition of 10 mM EDTA followed by heat inactivation at 75°C for 10 min. Digested DNA fragments were purified by ethanol precipitation prior to analysis. Undigested probes generated by PCR with unlabeled primers were used for sequencing reactions using 5′ FAM-labeled primers and a Thermo Sequenase dye primer manual sequencing kit (USB). Both digested fragments and sequencing reactions were resolved using a 3730xl DNA analyzer (Applied Biosystems) and then analyzed using GeneMapper software (Applied Biosystems).

Fluorescence polarization. N-terminal FITC-labeled synthetic peptides were kept constant in all reactions at a concentration of 1 μM. MBP-Rgg2 protein was serially diluted from 28 μM to 27 nM, and protein dilutions and peptide were mixed together to a final reaction volume of 50 μl in protein storage buffer (20 mM Tris-HCl buffer, pH 7.4; 200 mM NaCl, 1 mM EDTA, 20% [vol/vol] glycerol). Reaction mixtures were transferred to Corning 96-well half-area, black polystyrene plates preceding incubation at room temperature for 1 h. Polarization values were measured using a Polarstar Optima plate reader (BMG Labtech), and the resulting millipolarization unit (mP) values were plotted against protein concentration to assess protein-peptide interactions.

SUPPLEMENTAL MATERIAL

Supplemental material for this article may be found at http://mbio.asm.org/lookup/suppl/doi:10.1128/mBio.00333-12/-/DCSupplemental.

Figure S1, PDF file, 0.4 MB.
Figure S2, PDF file, 0.1 MB.
Figure S3, PDF file, 0.1 MB.
Figure S4, PDF file, 0.2 MB.
Figure S5, PDF file, 0.3 MB.
Figure S6, PDF file, 0.1 MB.
Table S1, PDF file, 0.2 MB.
Table S2, PDF file, 0.1 MB.
Table S3, PDF file, 0.2 MB.

ACKNOWLEDGMENTS

We thank Stephen Green and the UIC DNA Services Facility for their invaluable assistance in DNase I footprinting analysis by capillary electrophoresis and Jennifer Chang and Laura Cook for helpful comments on the manuscript and for sharing of strains.

This work was supported by a grant from the NIH NIAID, R01-AI091779, and the Hans W. Vahlteich Award.

REFERENCES

1. **Podbielski A, Kreikemeyer B.** 2004. Cell density—dependent regulation: basic principles and effects on the virulence of Gram-positive cocci. Int. J. Infect. Dis. **8**:81–95.
2. **Declerck N, et al.** 2007. Structure of PlcR: insights into virulence regulation and evolution of quorum sensing in Gram-positive bacteria. Proc. Natl. Acad. Sci. U. S. A. **104**:18490–18495.
3. **Rocha-Estrada J, Aceves-Diez AE, Guarneros G, de la Torre M.** 2010. The RNPP family of quorum-sensing proteins in Gram-positive bacteria. Appl. Microbiol. Biotechnol. **87**:913–923.
4. **Core L, Perego M.** 2003. TPR-mediated interaction of RapC with ComA inhibits response regulator-DNA binding for competence development in Bacillus subtilis. Mol. Microbiol. **49**:1509–1522.
5. **D'Andrea LD, Regan L.** 2003. TPR proteins: the versatile helix. Trends Biochem. Sci. **28**:655–662.
6. **Perego M, Brannigan JA.** 2001. Pentapeptide regulation of aspartyl-phosphate phosphatases. Peptides **22**:1541–1547.
7. **Shi K, et al.** 2005. Structure of peptide sex pheromone receptor PrgX and PrgX/pheromone complexes and regulation of conjugation in *Enterococcus faecalis*. Proc. Natl. Acad. Sci. U. S. A. **102**:18596–18601.
8. **Agaisse H, Gominet M, Okstad OA, Kolstø AB, Lereclus D.** 1999. PlcR is a pleiotropic regulator of extracellular virulence factor gene expression in *Bacillus thuringiensis*. Mol. Microbiol. **32**:1043–1053.
9. **Gohar M, et al.** 2008. The PlcR virulence regulon of *Bacillus cereus*. PLoS One **3**:e2793.
10. **Lereclus D, Agaisse H, Gominet M, Salamitou S, Sanchis V.** 1996. Identification of a *Bacillus thuringiensis* gene that positively regulates transcription of the phosphatidylinositol-specific phospholipase C gene at the onset of the stationary phase. J. Bacteriol. **178**:2749–2756.
11. **Slamti L, Lereclus D.** 2002. A cell-cell signaling peptide activates the PlcR virulence regulon in bacteria of the *Bacillus cereus* group. EMBO J. **21**:4550–4559.
12. **Kozlowicz BK, et al.** 2006. Molecular basis for control of conjugation by bacterial pheromone and inhibitor peptides. Mol. Microbiol. **62**:958–969.
13. **Bae T, Kozlowicz B, Dunny GM.** 2002. Two targets in pCF10 DNA for PrgX binding: their role in production of Qa and prgX mRNA and in regulation of pheromone-inducible conjugation. J. Mol. Biol. **315**:995–1007.
14. **Dunny GM, Johnson CM.** 2011. Regulatory circuits controlling enterococcal conjugation: lessons for functional genomics. Curr. Opin. Microbiol. **14**:174–180.
15. **Chatterjee A, et al.** 2011. Convergent transcription confers a bistable switch in *Enterococcus faecalis* conjugation. Proc. Natl. Acad. Sci. U. S. A. **108**:9721–9726.
16. **Chang JC, LaSarre B, Jimenez JC, Aggarwal C, Federle MJ.** 2011. Two Group A streptococcal peptide pheromones act through opposing Rgg regulators to control biofilm development. PLoS Pathog. **7**:e1002190.
17. **Fleuchot B, et al.** 2011. Rgg proteins associated with internalized small hydrophobic peptides: a new quorum-sensing mechanism in streptococci. Mol. Microbiol. **80**:1102–1119.

18. **Fontaine L, et al.** 2010. A novel pheromone quorum-sensing system controls the development of natural competence in *Streptococcus thermophilus* and *Streptococcus salivarius*. J. Bacteriol. **192**:1444–1454.
19. **Ibrahim M, et al.** 2007. Control of the transcription of a short gene encoding a cyclic peptide in *Streptococcus thermophilus*: a new quorum-sensing system? J. Bacteriol. **189**:8844–8854.
20. **Mashburn-Warren L, Morrison DA, Federle MJ.** 2010. A novel double-tryptophan peptide pheromone controls competence in streptococcus *spp*. via an Rgg regulator. Mol. Microbiol. **78**:589–606.
21. **Mashburn-Warren L, Morrison DA, Federle MJ.** 2012. The cryptic competence pathway in *Streptococcus pyogenes* is controlled by a peptide pheromone. J. Bacteriol. **194**:4589–4600.
22. **Sulavik MC, Tardif G, Clewell DB.** 1992. Identification of a gene, *rgg*, which regulates expression of glucosyltransferase and influences the Spp phenotype of *Streptococcus gordonii* Challis. J. Bacteriol. **174**:3577–3586.
23. **Karpenahalli MR, Lupas AN, Söding J.** 2007. TPRpred: a tool for prediction of TPR-, PPR- and SEL1-like repeats from protein sequences. BMC Bioinformatics **8**:2.
24. **Bortoni ME, Terra VS, Hinds J, Andrew PW, Yesilkaya H.** 2009. The pneumococcal response to oxidative stress includes a role for Rgg. Microbiology **155**:4123–4134.
25. **Chaussee MA, Callegari EA, Chaussee MS.** 2004. Rgg regulates growth phase-dependent expression of proteins associated with secondary metabolism and stress in *Streptococcus pyogenes*. J. Bacteriol. **186**:7091–7099.
26. **Chaussee MS, Ajdic D, Ferretti JJ.** 1999. The Rgg gene of *Streptococcus pyogenes* NZ131 positively influences extracellular SPE B production. Infect. Immun. **67**:1715–1722.
27. **Chaussee MS, Somerville GA, Reitzer L, Musser JM.** 2003. Rgg coordinates virulence factor synthesis and metabolism in *Streptococcus pyogenes*. J. Bacteriol. **185**:6016–6024.
28. **Chaussee MS, et al.** 2002. Rgg influences the expression of multiple regulatory loci to coregulate virulence factor expression in *Streptococcus pyogenes*. Infect. Immun. **70**:762–770.
29. **Dmitriev AV, et al.** 2006. The Rgg regulator of *Streptococcus pyogenes* influences utilization of nonglucose carbohydrates, prophage induction, and expression of the NAD-glycohydrolase virulence operon. J. Bacteriol. **188**:7230–7241.
30. **Fernandez A, Borges F, Gintz B, Decaris B, Leblond-Bourget N.** 2006. The rgg*C* locus, with a frameshift mutation, is involved in oxidative stress response by *Streptococcus thermophilus*. Arch. Microbiol. **186**:161–169.
31. **Fujiwara T, Hoshino T, Ooshima T, Sobue S, Hamada S.** 2000. Purification, characterization, and molecular analysis of the gene encoding glucosyltransferase from *Streptococcus oralis*. Infect. Immun. **68**:2475–2483.
32. **Pulliainen AT, Hytönen J, Haataja S, Finne J.** 2008. Deficiency of the Rgg regulator promotes H_2O2 resistance, AhpCF-mediated H_2O2 decomposition, and virulence in *Streptococcus pyogenes*. J. Bacteriol. **190**:3225–3235.
33. **Qi F, Chen P, Caufield PW.** 1999. Functional analyses of the promoters in the lantibiotic mutacin II biosynthetic locus in *Streptococcus mutans*. Appl. Environ. Microbiol. **65**:652–658.
34. **Rawlinson EL, Nes IF, Skaugen M.** 2002. LasX, a transcriptional regulator of the lactocin S biosynthetic genes in *Lactobacillus sakei* L45, acts both as an activator and a repressor. Biochimie **84**:559–567.
35. **Samen UM, Eikmanns BJ, Reinscheid DJ.** 2006. The transcriptional regulator RovS controls the attachment of *Streptococcus agalactiae* to human epithelial cells and the expression of virulence genes. Infect. Immun. **74**:5625–5635.
36. **Sanders JW, et al.** 1998. A chloride-inducible acid resistance mechanism in Lactococcus lactis and its regulation. Mol. Microbiol. **27**:299–310.
37. **Sulavik MC, Clewell DB.** 1996. Rgg is a positive transcriptional regulator of the *Streptococcus gordonii* gtfG gene. J. Bacteriol. **178**:5826–5830.
38. **Zheng F, et al.** 2011. Contribution of the Rgg transcription regulator to metabolism and virulence of *Streptococcus suis* serotype 2. Infect. Immun. **79**:1319–1328.
39. **Ibrahim M, et al.** 2007. A genome-wide survey of short coding sequences in streptococci. Microbiology **153**:3631–3644.
40. **Helmann JD.** 1995. Compilation and analysis of *Bacillus subtilis* sigma A-dependent promoter sequences: evidence for extended contact between RNA polymerase and upstream promoter DNA. Nucleic Acids Res. **23**:2351–2360.
41. **Browning DF, Busby SJ.** 2004. The regulation of bacterial transcription initiation. Nat. Rev. Microbiol. **2**:57–65.
42. **Loughman JA, Caparon MG.** 2007. Contribution of invariant residues to the function of Rgg family transcription regulators. J. Bacteriol. **189**:650–655.
43. **Dove SL, Darst SA, Hochschild A.** 2003. Region 4 of sigma as a target for transcription regulation. Mol. Microbiol. **48**:863–874.
44. **Shearwin KE, Callen BP, Egan JB.** 2005. Transcriptional interference—a crash course. Trends Genet. **21**:339–345.
45. **Howell-Adams B, Seifert HS.** 2000. Molecular models accounting for the gene conversion reactions mediating gonococcal pilin antigenic variation. Mol. Microbiol. **37**:1146–1158.
46. **Miroux B, Walker JE.** 1996. Over-production of proteins in *Escherichia coli*: mutant hosts that allow synthesis of some membrane proteins and globular proteins at high levels. J. Mol. Biol. **260**:289–298.
47. **Charpentier E, et al.** 2004. Novel cassette-based shuttle vector system for gram-positive bacteria. Appl. Environ. Microbiol. **70**:6076–6085.
48. **Zianni M, Tessanne K, Merighi M, Laguna R, Tabita FR.** 2006. Identification of the DNA bases of a DNase I footprint by the use of dye primer sequencing on an automated capillary DNA analysis instrument. J. Biomol. Tech. **17**:103–113.